Supplementary information for

Coupling Biomass Carbon Engineering with Phosphorus Chemistry for High-Performance Flexible Zinc-Ion Hybrid Supercapacitors

*Himanshu Gupta [a], Anusree S. Chandran [b], Nishant Shukla [c], Manikantan R. Nair [b], Muruganandham Hariram [a], Rudransh Dev [a], Dinesh K. Shukla [d], Vasant G. Sathe [d], Manoj Kumar [a], Tribeni Roy [b], Debasish Sarkar [a,]**

[a] Department of Physics, Malaviya National Institute of Technology Jaipur, Rajasthan, 302017, India

[b] Department of Mechanical Engineering, Birla Institute of Technology and Science Pilani, Pilani, Rajasthan 333031, India

[c] Department of Physics, The Assam Kaziranga University, Jorhat, 785006, Assam, India

[d] UGC-DAE Consortium for Scientific Research, University Campus, Khandwa Road, Indore, 452001, India

*Corresponding Authors

E-mail: debasish.phy@mnit.ac.in (D. Sarkar)

Computation of specific capacity, energy and power densities for ZIHSC-

The specific capacitance (C_s, measured in F/g) is determined using the discharge data of the galvanostatic charge-discharge curves (GCD) and area of the CV curve through the application of the following equation:

Specific capacitance: $C_s = \frac{i * \Delta t}{m * \Delta V}$ (using GCD curves)

Specific capacitance: $C_s = \frac{\int i\,(V)\,dV}{2\,m * v * \Delta V}$ (using CV curves)

Where i (A) is the current, Δt (s) is the discharge time for potential window ΔV (V), m (g) is the mass of the active material on the cathode, $\int i\,(V)\,dV$ is the are enclosed by the CV curve (A.V), and v is the scan rate (V/s).

The energy density (E, Wh/kg) and power density (W/kg) of ZIHSC are calculated using these equations:

Energy density: $E = \frac{1}{2 * 3.6} C_s \Delta V^2$

Power density: $P = \frac{3600 * E}{\Delta t}$

Where, C_s (F/g) is the specific capacitance, ΔV (V) is the operating potential window, and Δt (s) is the discharge time.

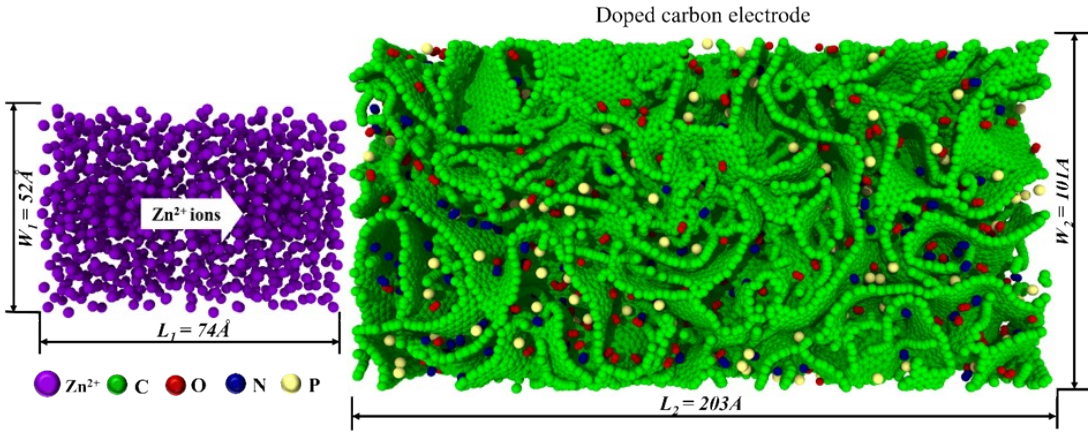

Fig. S1 Snapshot of the simulation box packed with doped porous carbon electrode (right) and Zn^{2+} ions (left) for the MD simulation.

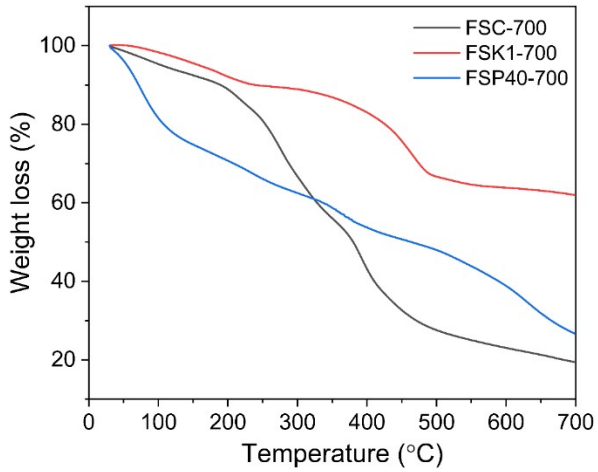

Fig. S2 TGA of different FS-derived carbon samples.

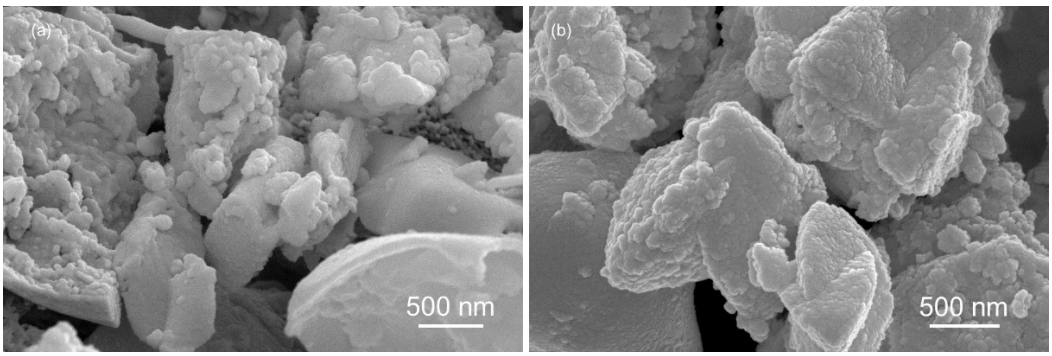

Fig. S3 FESEM images of fennel-seed derived (a) pristine FSC-700 and (b) KOH activated FSK1-700 carbon samples.

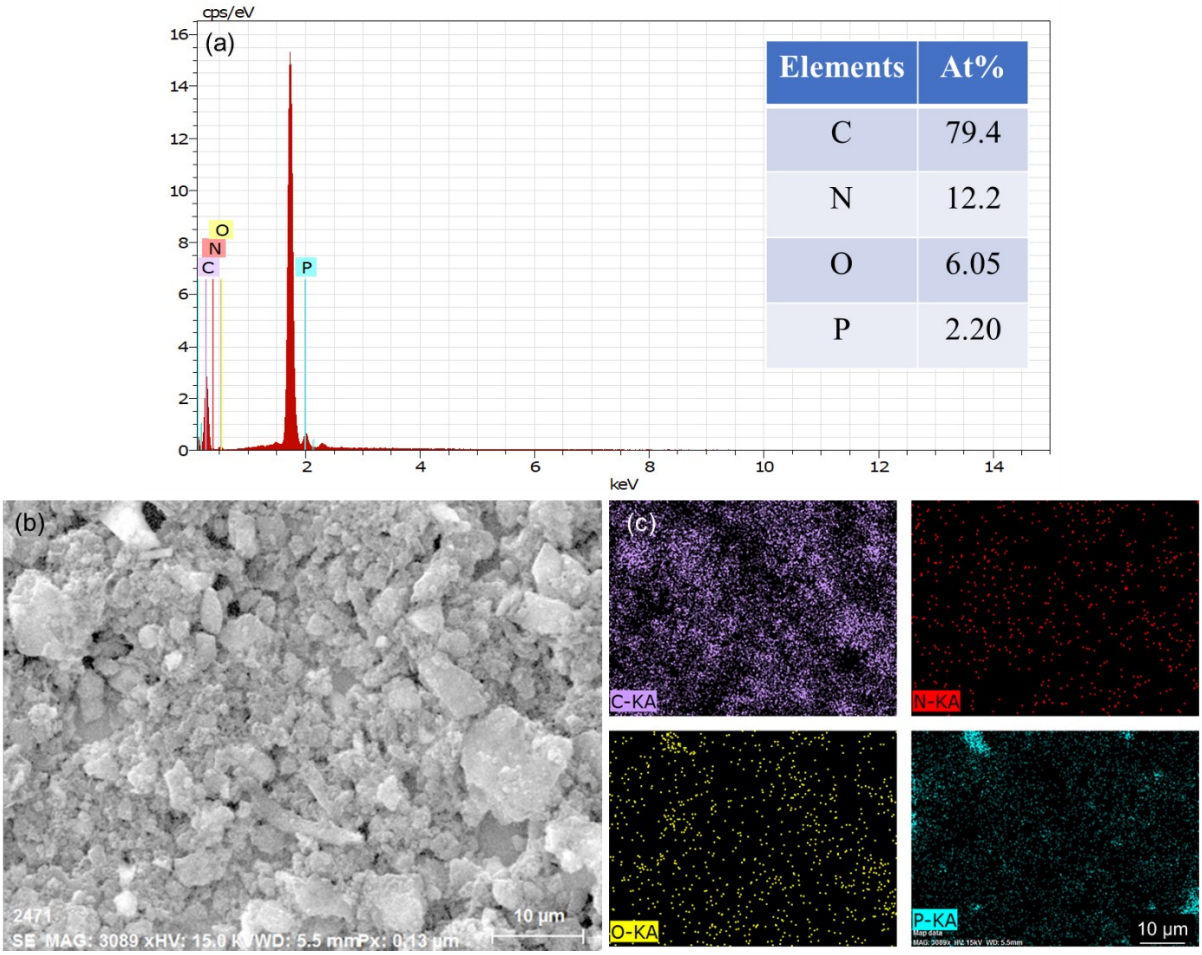

Fig. S4 (a) EDS spectrum of FSP40-700, (b) mapping region in FESEM, and (c) mapping of different constituent elements, C, N, O, and P.

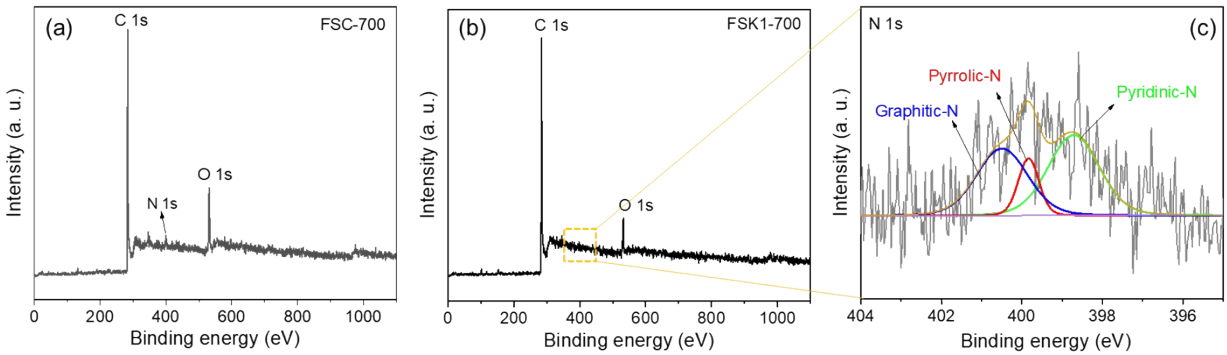

Fig. S5 XPS survey spectra of (a) FSC-700 and (b) FSK1-700 samples, and (c) high-resolution deconvoluted XPS spectra of N 1s for FSK1-700 sample.

Table S1. Atomic percentage of different elements present in different samples estimated using XPS technique -

Sl. No.	Sample name	C (at. %)	O (at. %)	N (at. %)	P (at. %)
1.	FSC-700	86.6	11.35	2.05	-
2.	FSK1-700	92.77	5.57	1.66	-
3.	FSP40-700	90.14	5.47	2.54	1.85

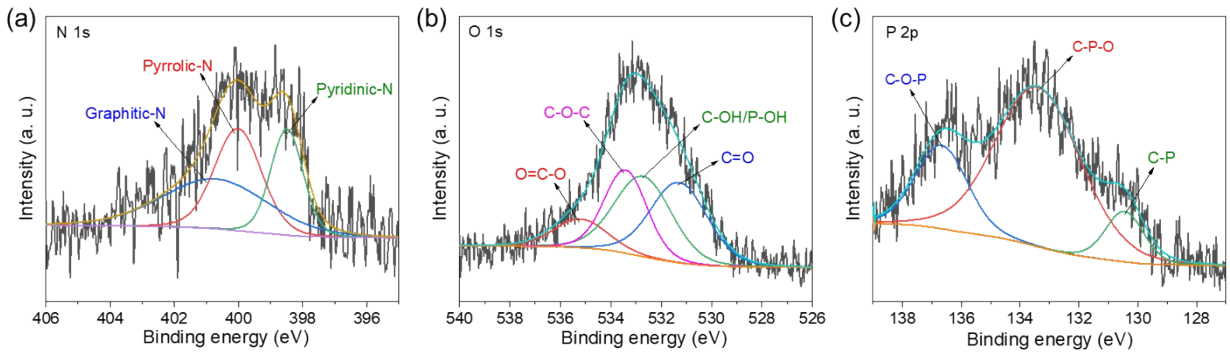

Fig. S6 High-resolution XPS spectrum of (a) N 1s, (b) O 1s and (c) P 2p for FSP40-700 sample.

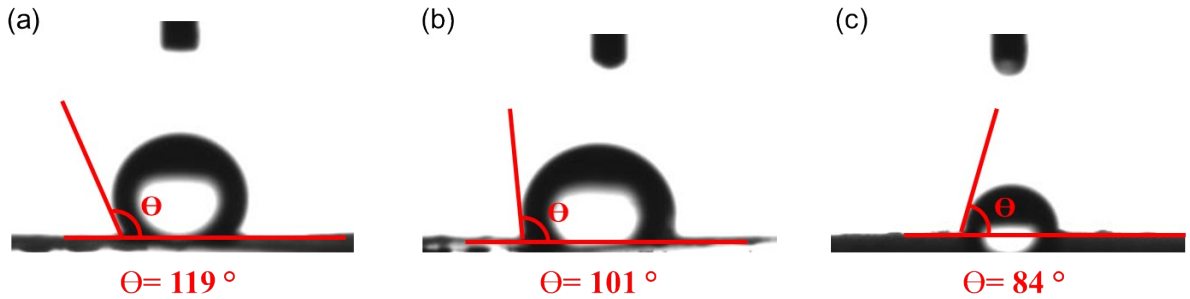

Fig. S7 Contact angle analysis results of samples: (a) FSC-700, (b) FSK1-700, and (c) FSP40-700.

Table S2 Specific surface areas (SSA) of KOH-activated porous carbons derived from different biomasses -

Sl. No.	Carbon precursor	Activating agent	SSA (m^2/g)	Ref.
1.	Lignin	KOH	652	[1]
2.	Feather finger grass flower	KOH	637	[2]
3.	Waste newspaper	KOH	416	[3]
4.	Lotus calyx biowaste	KOH	798	[4]
5.	Wheat straw cellulosic foam	KOH	772	[5]
6.	Sorghum waste	KOH	948	[6]
7.	Sawdust of Oak, hornbeam, apple, and cherry	KOH	672-912	[7]
8.	Pencil shavings (activated at different temperatures)	KOH	598-1293	[8]
9.	Bamboo	KOH	414	[9]
10.	Waste lemon peels	KOH	2276	[10]
11.	Bitter apple pulp	KOH	3254	[11]
12.	Coconut shells	KOH	3512	[12]

Table S3 Specific surface area (SSA) and pore volumes of different carbon samples-

Sl. No.	Sample	S_{BET} (m^2/g)	Average Pore size (nm)	Pore volume (cm^3/g)	Micropore S_{BET} (m^2/g)	Meso & macropore S_{BET} (m^2/g)
1.	FSC-700	24	8.34	0.05	2.8	21.2
2.	FSK1-700	587	2.60	0.38	191	396
3.	FSP40-700	650	3.66	0.59	140	510

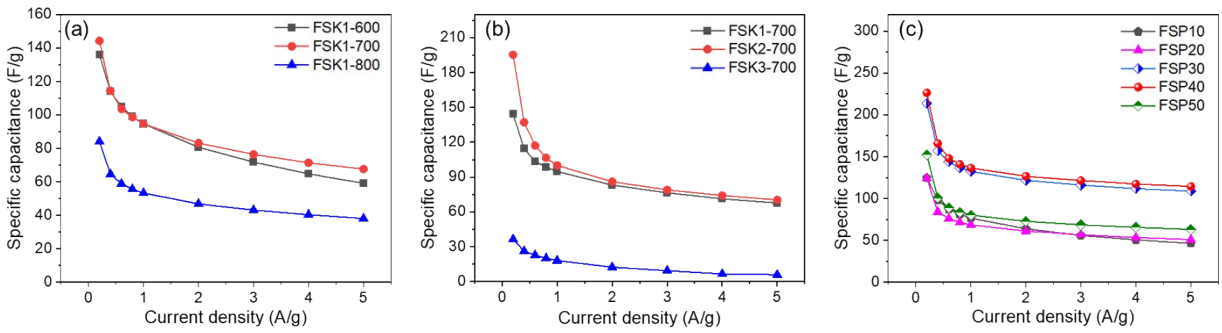

Fig. S8 Specific capacitance versus current density plots for- (a) carbon samples activated at different temperatures with KOH to FS-powder ratio 1:1; (b) carbon samples activated at 700 °C with different KOH to FS-powder ratios (1:1, 2:1, and 3:1), and (c) carbon samples activated at 700 °C with different H_3PO_4 concentrations (wt. %) in FS-powder.

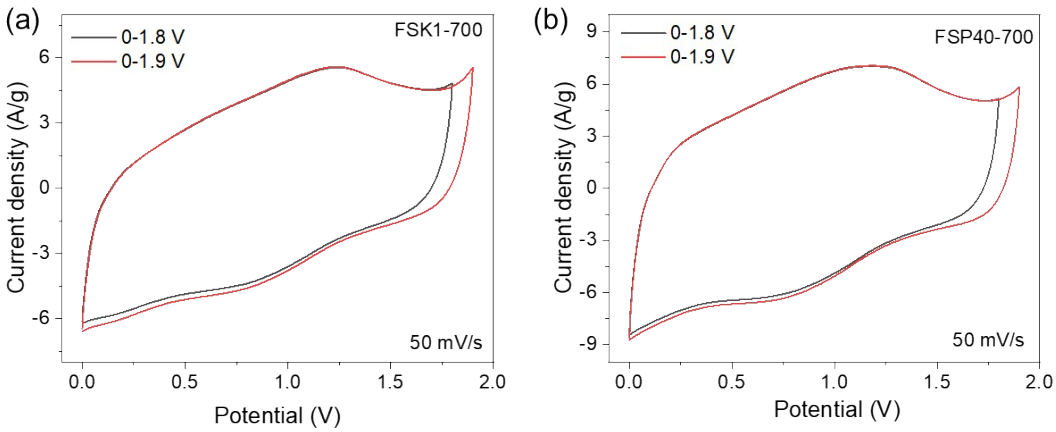

Fig. S9 CVs of ZIHSC half-cells within different potential windows with: (a) FSK1-700, (b) FSP40-700 cathodes and 2M $ZnSO_4$ electrolyte.

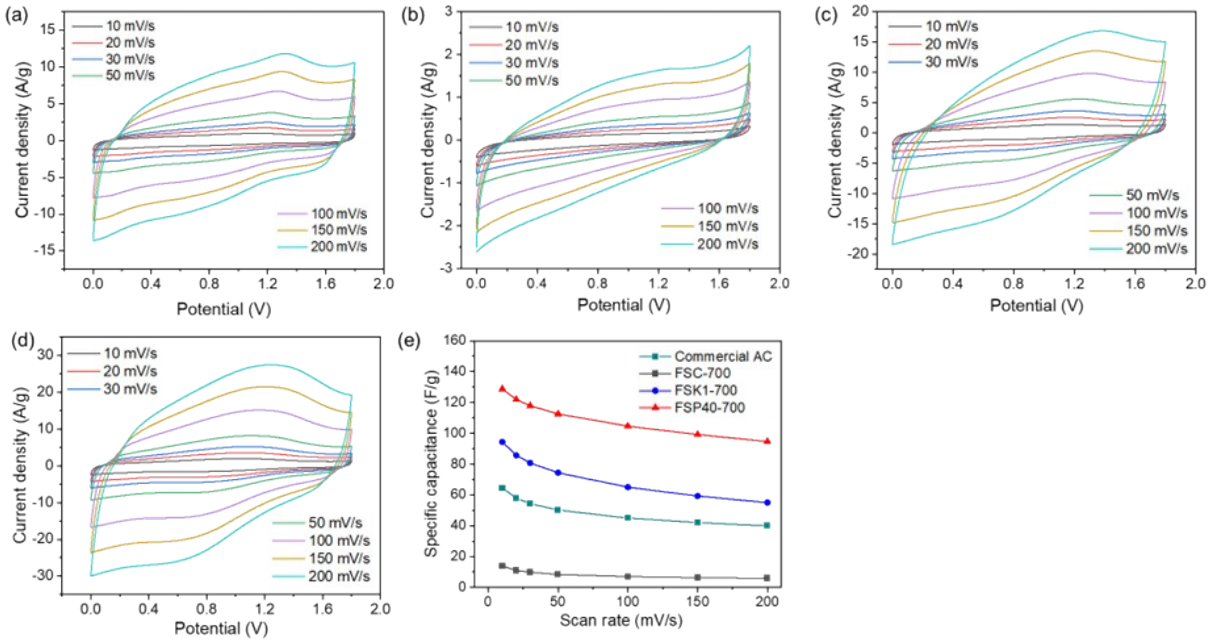

Fig. S10 Cyclic voltammograms at different scan rates for ZIHSCs with (a) Commercial AC, (b) FSC-700, (c) FSK1-700, (d) FSP40-700 based cathodes; and (e) variation of specific capacitance with scan rates for different carbon materials.

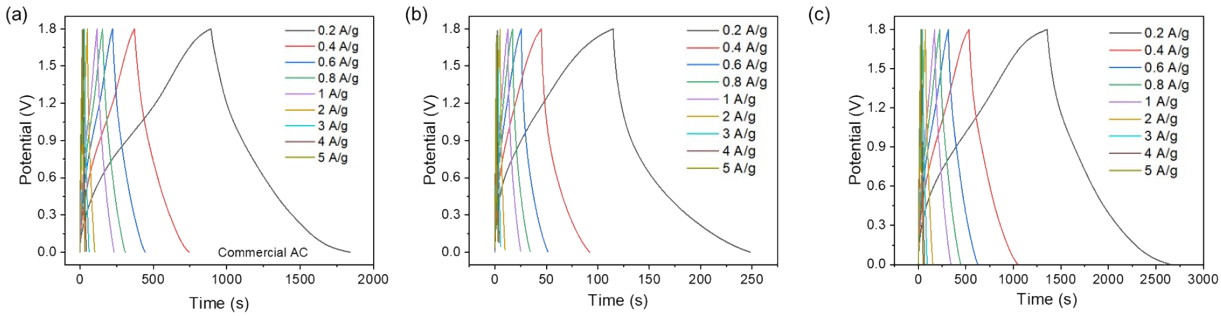

Fig. S11 GCD profiles at different current densities for ZIHSCs with (a) Commercial AC, (b) FSC-700 and (c) FSK1-700 based cathodes.

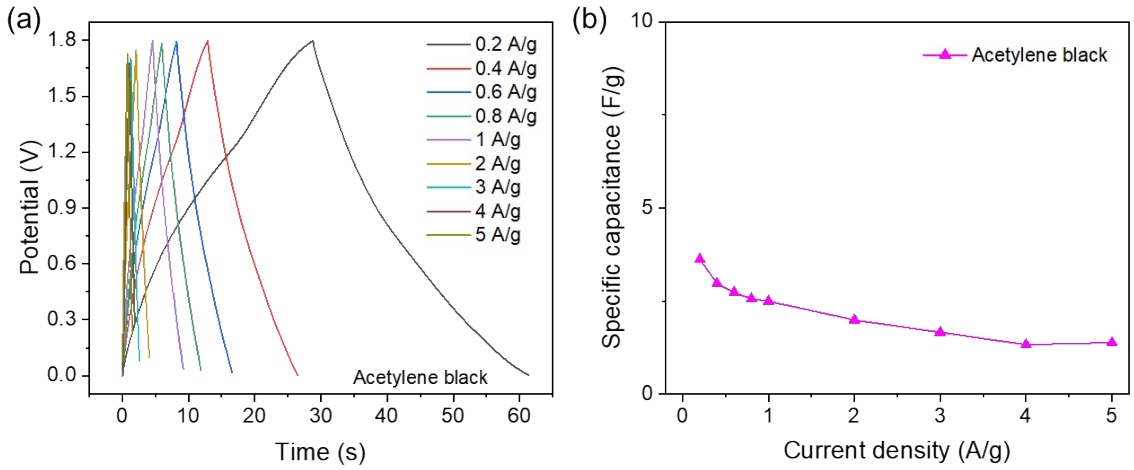

Fig. S12 For Zn//acetylene black ZIHSC: (a) GCD profiles and (b) Specific capacitance at different current densities.

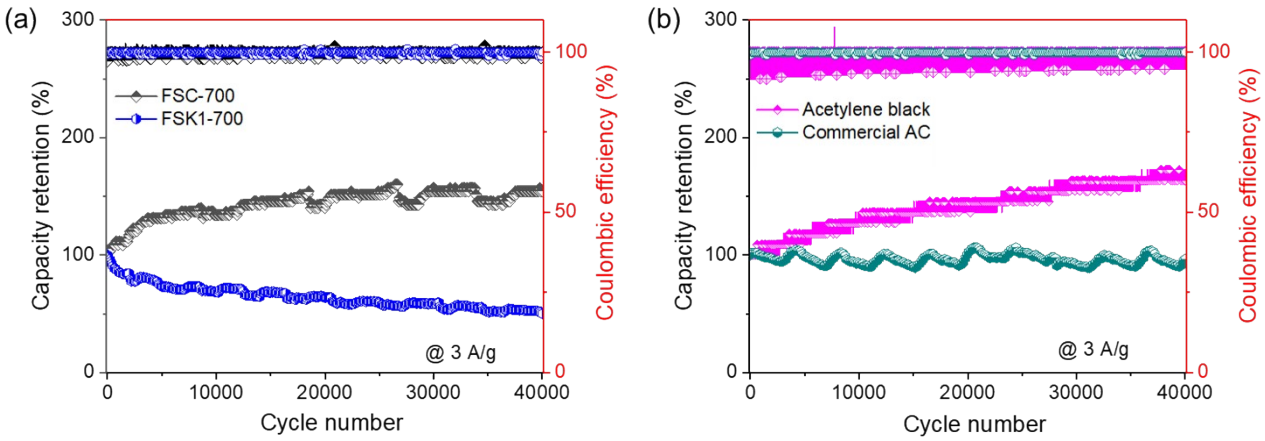

Fig. S13 Cycling stability of different control samples used to assemble ZIHSCs in this study.

Table S4 Electrochemical performance comparison of different carbon-based cathode materials in aqueous ZIHSCs-

Sl. No.	Cathode material	Activating agent	SSA (m^2/g)	Electrolyte	Potential window (V)	Capacity (mAh/g)	Energy density (Wh/kg)	Power density (kW/kg)	Ref.
1.	**FSP40-700**	**H_3PO_4**	**650**	**2M $ZnSO_4$**	**0-1.8**	**113 (0.2 A/g)**	**102**	**0.18**	**This work**
2.	**FSK1-700**	**KOH**	**587**	**2M $ZnSO_4$**	**0-1.8**	**72 (0.2 A/g)**	**64**	**0.18**	**This work**
3.	BH-4	-	-	2M $ZnSO_4$	0.2-1.8	132 (1 A/g)	117.5	0.89	[13]
4.	PBC-A900	KOH	414	$Zn(CF_3SO_3)_2$	0.2-1.8	142.8 (1 A/g)	114	0.8	[9]
5.	NSCNS	$K_2S_2O_8$	2110	2M $ZnSO_4$	0.2-1.8	141.5 (0.1 A/g)	113.4	0.075	[14]
6.	N, O-HPC	-	-	2M $ZnSO_4$	0.2-1.8	138.5 (0.5 A/g)	110	0.138	[15]
7.	HNPC	NH_3	-	1M $ZnSO_4$	0-1.8	177.8 (4.2 A/g)	107.3	-	[16]
8.	N, S-PCD	-	924	2M $ZnSO_4$	0.2-1.8	133.4 (0.2 A/g)	106.7	0.016	[17]
9.	AC-850	KOH	2156	1M $ZnSO_4$	0-1.8	125.7 (1 A/g)	104.4	0.095	[18]
10.	NPG	-	168	1M $ZnSO_4$	0-1.8	105.1 (0.5 A/g)	94.6	0.44	[19]
11.	AC	commercial	1923	2M $ZnSO_4$	0.2-1.8	121 (0.1 A/g)	84	-	[20]
12.	PCM-800	NaOH	477	$C_6F_6O_6S_2Zn$	0-1.9	113.3 (0.1 A/g)	64.9	0.028	[21]
13.	NSPCN-800	$Na_2S_2O_3$	1297	2M $ZnSO_4$	0.2-1.8	95.2 (0.1 A/g)	59	0.041	[22]
14.	RHC-850	Na_2CO_3-K_2CO_3	1012	3M $Zn(CF_3SO_3)_2$	0.1-1.8	70.7 (0.2 A/g)	58	0.169	[23]
15.	HMFC	KOH	2637	2M $ZnSO_4$	0.2-1.8	132 (0.1 A/g)	95.2	0.074	[24]
16.	S-MCF-N	-	-	$Zn(CF_3SO_3)_2$	0.2-1.8	92.4 (0.2 A/g)	72.4	0.15	[25]
17.	NS-ONC	-	-	2M $ZnSO_4$	0-1.8	55.5 (0.5 A/g)	50	0.45	[26]
18.	MSCP	NaCl-$NaNO_3$	499	2M $ZnSO_4$	0-1.8	68.2 (0.68 A/g)	36.5	0.376	[27]
19.	BP-H_3PO_4	H_3PO_4	218	2M $ZnSO_4$	0-2.0	122.7 (0.1 A/g)	120	0.11	[28]
20.	BG-H_3PO_4	H_3PO_4	129	2M $ZnSO_4$	0.2-1.8	138.6 (0.1 A/g)	104.6	0.1	[29]
21.	GS-H_3PO_4	H_3PO_4	617	2M $ZnSO_4$	0.2-1.8	65.2 (0.1 A/g)	50.2	0.1	[30]
22.	BAPC1-900	KOH	3254	2M $ZnSO_4$	0-1.8	180 (0.5A/g)	162	0.45	[11]
23.	NS-LPC-850	KOH	2276	6M KOH+0.35M ZnO	0.4-1.4	102 (1 A/g)	67	1	[10]

Table S5 EIS fitted parameters-

Sl. No.	Sample	R_s (Ω)	R_{ct} (Ω)
1.	FSC-700	4.2	484
2.	FSK1-700	4.5	190
3.	FSP40-700	2.7	150

Dunn's method of extracting capacitive and diffusive charges from CVs recorded at different scan rates-

The peak current in the CVs and scan rates obey the following power law:

$$i = av^b$$

Here, *a* & *b* are two adjustable parameters. A process that stores charge through diffusion-controlled is indicated by *b* = 0.5. while a value of *b* = 1 refers to 'capacitive' processes. The slope of the straight-line plot of log(*i*) versus log(*v*) at different charge-discharge voltages can be used to calculate *b*-values. Now, due to the difference in scan rate dependence, the contributions of capacitive and diffusive processes can be mathematically separated. Dunn and coworkers detailed the procedure in the literature.[31, 32] To put it succinctly, this technique uses the following equation to simplify the diffusion-controlled and capacitive contributions to the current *i*(V) at a given voltage:

$$i(V) = a_1 v + a_2 v^{1/2}$$

The above equation can be rearranged as follows:

$$i(V)/v^{1/2} = a_1 v^{1/2} + a_2$$

The slopes and intercepts, a_1 and a_2, can now be determined by plotting the straight lines $i(V)/v^{1/2}$ vs. $v^{1/2}$ at various voltages. At certain potentials, the current contributions from diffusive ($a_2 v^{1/2}$) and capacitive ($a_1 v$) processes can then be determined.[33]

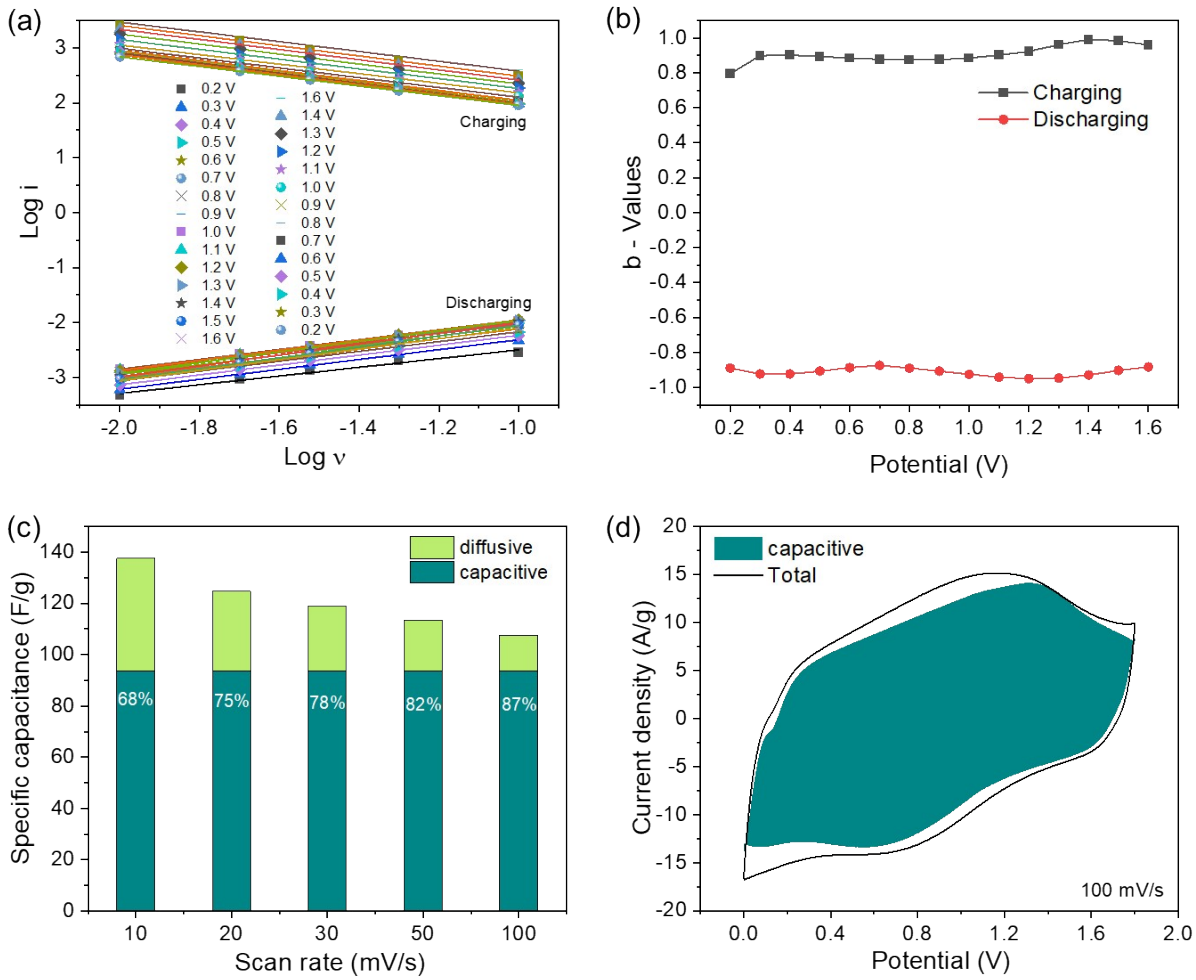

Fig. S14 Charge storage kinetics analysis of Zn//FSP40-700 based ZIHSC: (a) Log *i* vs Log *v* plots and (b) evaluated *b*-values at different charge-discharge voltages, (c) Segregation of diffusive and capacitive contributions to the total capacitance at different scan rates, and (d) plot of capacitive current to the total current in the CV measured at 100 mV/s.

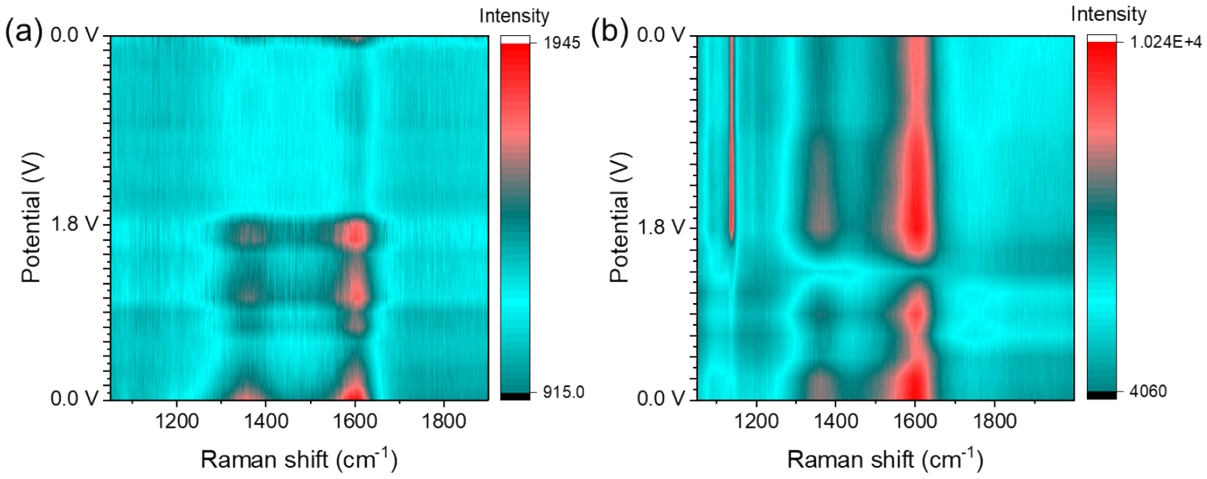

Fig. S15 In-situ Raman spectral analysis of (a) FSC-700 and (b) FSK1-700 based ZIHSCs with aqueous 2M $ZnSO_4$ electrolyte.

Table S6 Key distances from the optimized complexes (Å)

Complex	Shortest contact
Pristine graphene + Zn^{2+}	Zn···C = 3.562; Zn height above C-plane = 3.067
O, N-doped graphene + Zn^{2+}	Zn–O = 1.99189
O, N, P-doped graphene + Zn^{2+}	Zn–O(P) = 1.99126

Table S7 Dipole moments of the adsorbed complexes (Debye)

Complex	Dipole Tot (D)
Pristine graphene + Zn^{2+}	4.3054
O, N-doped graphene + Zn^{2+}	7.0754
O, N, P-doped graphene + Zn^{2+}	7.6928

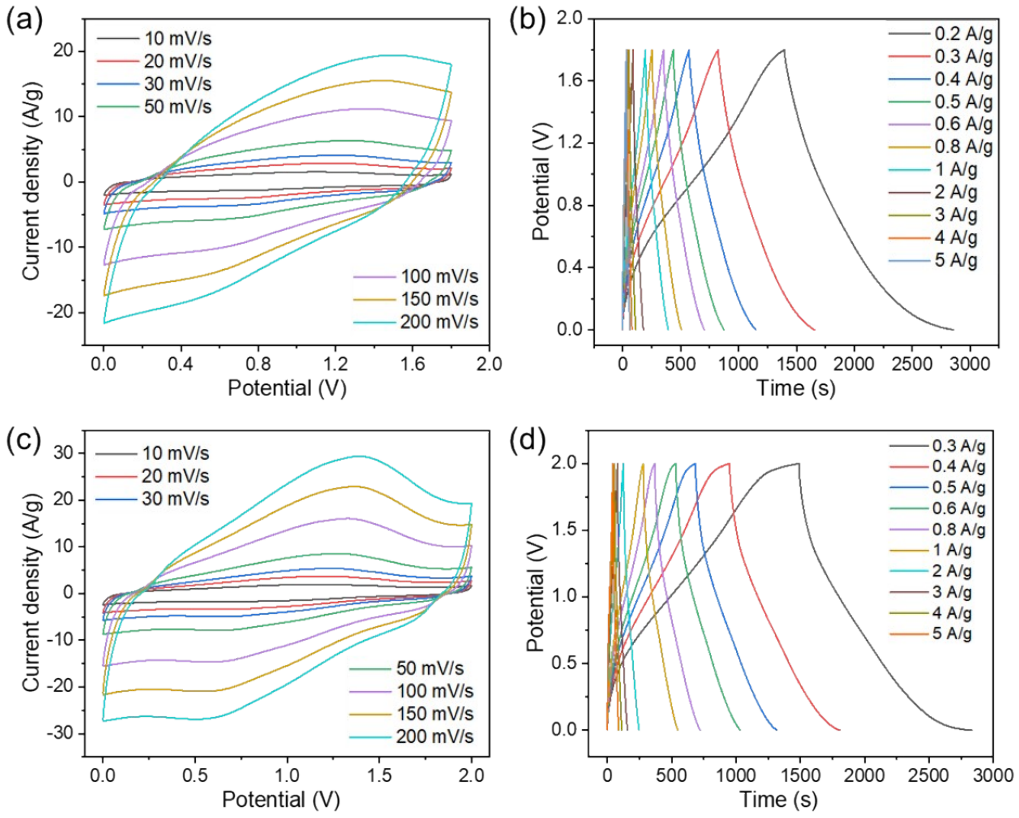

Fig. S16 CVs at different scan rates and GCD profiles at different current densities recorded for f-ZIHSC within (a-b) 0-1.8 V and (c-d) 0-2.0 V voltage windows.

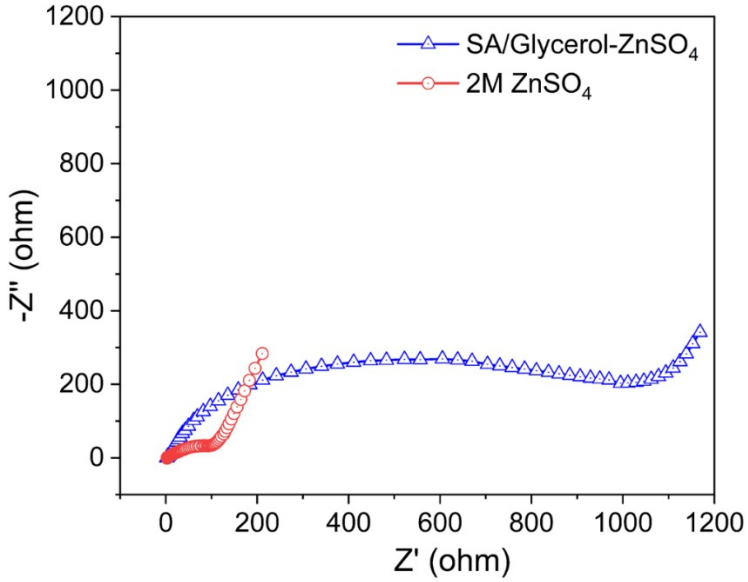

Fig. S17 EIS comparison of aqueous and hydrogel-based ZIHSCs.

Table S8 Electrochemical performance comparison of FSP40-700-based flexible ZIHSC (f-ZIHSC) device with other carbon-based f-ZIHSC systems reported in recent literatures-

Sl. No.	Cathode material	Electrolyte	Potential window (V)	Capacity (mAh/g)	Energy density (Wh/kg)	Power density (kW/kg)	Ref.
1.	**FSP-40-700**	**SA/Glycerol-$ZnSO_4$ gel**	**0-1.8**	**69 @ 0.3 A/g**	**72.9**	**0.18**	**This work**
2.	**FSP-40-700**	**SA/Glycerol-$ZnSO_4$ gel**	**0-2.0**	**123 @ 0.3 A/g**	**123**	**0.33**	**This work**
3.	HCS	PAM hydrogel	0.15-1.95	86 @ 0.5 A/g	59.7	0.44	[34]
4.	BC-CNa	PAM gel	0.2-1.8	48 @ 0.2 A/g	35.9	0.14	[35]
5.	CNPK	PVA/$ZnAC_2$/KOH gel	0.2-1.8	141 @ 0.1 A/g	89.3	0.079	[36]
6.	NPFC	$Zn(CF_3SO_3)_2$/PAM hydrogel	-	163..6 @ 0.1 A/g	60.1	0.074	[37]
7.	WC-6ZnN-12U	PAM-$ZnSO_4$	0.2-1.8	34.6 @ 0.1 A/g	27.7	0.035	[38]
8.	LDC	Gelatin/$ZnSO_4$ gel	0.2-1.8	116.8 @ 0.5 A/g	86.8	0.42	[39]
9.	PBC-A900	PVA-$Zn(CF_3SO_3)_2$	0.2-1.8	155 @ 0.8 A/g	107	0.8	[8]

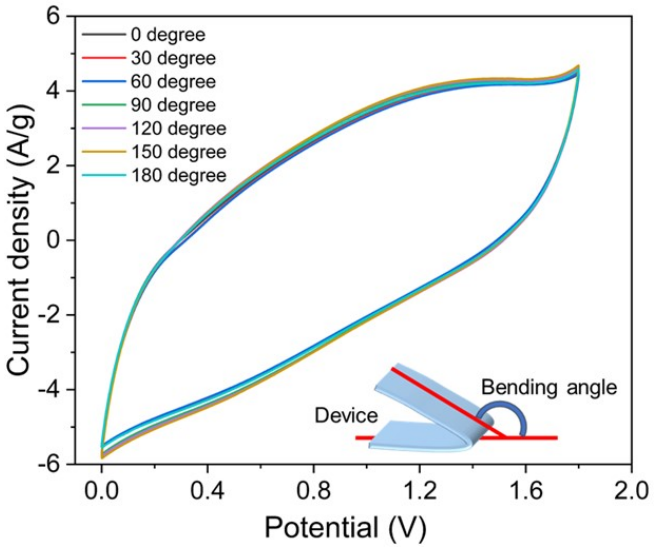

Fig. S18 CV curves recorded at different bending angles of the assembled gel-electrolyte-based f-ZIHSC with FSP40-700 as cathode material.

References

1. C. Li, Y. Li, Y. Shao, L. Zhang, S. Zhang, S. Wang, B. Li, Z. Cui, Y. Tang and X. Hu, *Green Chemistry*, 2023, **25**, 2825-2839.
2. R. A. Senthil, V. Yang, J. Pan and Y. Sun, *J. Energy Storage*, 2021, **35**, 102287.
3. D. Kalpana, S. H. Cho, S. B. Lee, Y. S. Lee, R. Misra and N. G. Renganathan, *J. Power Sources*, 2009, **190**, 587-591.
4. G. Dhakal, D. Mohapatra, Y.-I. Kim, J. Lee, W. K. Kim and J.-J. Shim, *Renewable Energy*, 2022, **189**, 587-600.
5. G. Gou, F. Huang, M. Jiang, J. Li and Z. Zhou, *Renewable Energy*, 2020, **149**, 208-216.
6. J. Hou, Y. Liu, S. Wen, W. Li, R. Liao and L. Wang, *ACS Omega*, 2020, **5**, 13548-13556.
7. K. Jedynak and B. Charmas, *Adsorption*, 2024, **30**, 167-183.
8. Z. Li, D. Chen, Y. An, C. Chen, L. Wu, Z. Chen, Y. Sun and X. Zhang, *Energy Storage Mater.*, 2020, **28**, 307-314.
9. J. Wang, Y. Huang, X. Han, Z. Li, S. Zhang and M. Zong, *Appl. Surf. Sci.*, 2022, **579**, 152247.
10. F. Ullah, I. Shahid, Y. Sun, R. Andavar, U. A. Kolachi, Z. Zhu and J. Pan, *Nanoscale*, 2025, **17**, 27011-27024.
11. H. Gupta, H. K. Rathore, M. Kumar, P. W. Menezes and D. Sarkar, *Small*, 2025, **21**, 2502071.
12. B. Hou, T. Zhang, R. Yan, D. Li, Y. Mo, L. Yin and Y. Chen, *Int. J. Electrochem. Sci.*, 2016, **11**, 9007-9018.
13. H. Fan, S. Zhou, Q. Li, G. Gao, Y. Wang, F. He, G. Hu and X. Hu, *J. Colloid Interface Sci.*, 2021, **600**, 681-690.
14. D. Wang, S. Wang and J. Sun, *Biomass Conv. Bioref.*, 2024, **14**, 7031-7043.
15. X. Deng, J. Li, Z. Shan, J. Sha, L. Ma and N. Zhao, *J. Mater. Chem. A*, 2020, **8**, 11617-11625.
16. H. Zhang, Q. Liu, Y. Fang, C. Teng, X. Liu, P. Fang, Y. Tong and X. Lu, *Adv. Mater.*, 2019, **31**, 1904948.
17. Y. Yang, D. Chen, H. Wang, P. Ye, Z. Ping, J. Ning, Y. Zhong and Y. Hu, *Chem. Eng. J.*, 2022, **431**, 133250.
18. J. Yu, L. Wang, J. Peng, X. Jia, L. Zhou, N. Yang and L. Li, *Ionics*, 2021, **27**, 4495-4505.

19. Y. Zhao, H. Hao, T. Song, X. Wang, C. Li and W. Li, *J. Power Sources*, 2022, **521**, 230941.
20. L. Dong, X. Ma, Y. Li, L. Zhao, W. Liu, J. Cheng, C. Xu, B. Li, Q.-H. Yang and F. Kang, *Energy Storage Mater.*, 2018, **13**, 96-102.
21. X. Zhang, E. Cao, Y. Tian, M. Zhang, X. Liu, Z. Lei, Z. Zhao, P. Cui, Q. Ling and R. Xie, *Carbon Resour. Convers.*, 2022, **5**, 193-199.
22. P. Song, C. Li, N. Zhao, Z. Ji, L. Zhai, X. Shen and Q. Liu, *J. Colloid Interface Sci.*, 2023, **633**, 362-373.
23. Y. Liu, H. Tan, Z. Tan and X. Cheng, *Appl. Surf. Sci.*, 2023, **608**, 155215.
24. F. Kang, Y. Li, Z. Zheng, X. Peng, J. Rong and L. Dong, *J. Colloid Interface Sci.*, 2024, **669**, 766-774.
25. J. Hong and C. Jo, *J. Power Sources*, 2024, **594**, 234006.
26. R. Aggarwal, H. Gupta, K. Awasthi, M. Kumar, D. Sarkar and S. K. Sonkar, *Langmuir*, 2024, **40**, 9481-9489.
27. S. Zeng, X. Shi, D. Zheng, C. Yao, F. Wang, W. Xu and X. Lu, *Mater. Res. Bull.*, 2021, **135**, 111134.
28. M. Gautam, T. Patodia, V. Gupta, K. Sachdev and H. S. Kushwaha, *J. Energy Storage*, 2024, **102**, 114088.
29. M. Gautam, T. Patodia, K. Sachdev and H. S. Kushwaha, *Biomass Conv. Bioref.*, 2025, **15**, 6389-6400.
30. M. Gautam, T. Patodia, P. Kushwaha, M. Agrawal, K. Sachdev and H. S. Kushwaha, *Carbon Trends*, 2024, **15**, 100341.
31. H.-S. Kim, J. B. Cook, H. Lin, Jesse S. Ko, Sarah H. Tolbert, V. Ozolins and B. Dunn, *Nat. Mater.*, 2017, **16**, 454-460.
32. J. Wang, J. Polleux, J. Lim and B. Dunn, *J. Phys. Chem. C*, 2007, **111**, 14925-14931.
33. D. Sarkar, D. Das, S. Das, A. Kumar, S. Patil, K. K. Nanda, D. D. Sarma and A. Shukla, *ACS Energy Lett.*, 2019, **4**, 1602-1609.
34. S. Chen, L. Ma, K. Zhang, M. Kamruzzaman, C. Zhi and J. A. Zapien, *J. Mater. Chem. A*, 2019, **7**, 7784-7790.
35. H. Chen, Y. Zheng, X. Zhu, W. Hong, Y. Tong, Y. Lu, G. Pei, Y. Pang, Z. Shen and C. Guan, *Mater. Res. Bull.*, 2021, **139**, 111281.
36. H. Zhang, Z. Chen, Y. Zhang, Z. Ma, Y. Zhang, L. Bai and L. Sun, *J. Mater. Chem. A*, 2021, **9**, 16565-16574.
37. F. Wei, Y. Wei, J. Wang, M. Han and Y. Lv, *Chem. Eng. J.*, 2022, **450**, 137919.

38. G. Lou, G. Pei, Y. Wu, Y. Lu, Y. Wu, X. Zhu, Y. Pang, Z. Shen, Q. Wu, S. Fu and H. Chen, *Chem. Eng. J.*, 2021, **413**, 127502.
39. Y. Lu, Z. Li, Z. Bai, H. Mi, C. Ji, H. Pang, C. Yu and J. Qiu, *Nano Energy*, 2019, **66**, 104132.